

Tensor meson excitation in the reaction $\gamma\gamma \rightarrow K_S^0 K_S^0$

PLUTO Collaboration

Ch. Berger, H. Genzel, W. Lackas, J. Pielorz¹,
F. Raupach, W. Wagner²

I. Phys. Institut der RWTH Aachen³, D-5100 Aachen,
Federal Republic of Germany

A. Klovning, E. Lillestøl
University of Bergen⁴, N-5014 Bergen, Norway

J. Bürger, L. Criegee, A. Deuter, F. Ferrarotto⁵,
G. Franke, M. Gaspero⁵, Ch. Gerke, G. Knies,
B. Lewendel⁶, J. Meyer, U. Michelsen, K.H. Pape,
B. Stella⁵, U. Timm, G.G. Winter, M. Zachara⁷,
W. Zimmermann

Deutsches Elektronen-Synchrotron DESY, D-2000 Hamburg,
Federal Republic of Germany

P.J. Bussey, S.L. Cartwright⁸, J.B. Dainton⁹,
D. Hendry, B.T. King⁹, C. Raine, J.M. Scarr,
I.O. Skillicorn, K.M. Smith, J.C. Thomson
University of Glasgow¹⁰, Glasgow G12 8QQ, UK

Received 6 August 1987; in revised form 20 October 1987

¹ Deceased

² Present address: University of California at Davis, Davis,
CA 95616, USA

³ Supported by the BMFT, FRG

⁴ Partially supported by the Norwegian Council for Science and
the Humanities

⁵ Rome University, partially supported by I.N.F.N., Sezione di
Roma, I-00135 Rome, Italy

⁶ Present address: I. Institut für Experimentalphysik der Univer-
sität Hamburg, D-2000 Hamburg, FRG

⁷ Institute of Nuclear Physics, PL-30059 Cracow, Poland

⁸ Present address: SLAC, Stanford, USA

⁹ Present address: University of Liverpool, Liverpool, L69 3BX, UK

¹⁰ Supported by the UK. Science and Engineering Research Council

¹¹ Present address: Carleton University, Ottawa, Ontario, Canada
K1S 5B6

O. Achterberg, V. Blobel, D. Burkart,
K. Diehlmann, M. Feindt, H. Kapitzka¹¹,
B. Koppitz, M. Krüger¹², M. Poppe¹³, H. Spitzer,
R. van Staa

II. Institut für Experimentalphysik der Universität Hamburg³,
D-2000 Hamburg, Federal Republic of Germany

C.Y. Chang, R.G. Glasser, R.G. Kellogg,
S.J. Maxfield¹⁴, R.O. Polvado, B. Sechi-Zorn¹,
J.A. Skard, A. Skuja, A.J. Tylka¹⁵, G.E. Welch¹⁶,
G.T. Zorn

University of Maryland¹⁷, College Park, MD 20742, USA

F. Almeida¹⁸, A. Bäcker, F. Barreiro¹⁹, S. Brandt,
K. Derikum²⁰, C. Grupen, H.J. Meyer, H. Müller,
B. Neumann, M. Rost, K. Stupperich, G. Zech

Universität-Gesamthochschule Siegen³, D-5900 Siegen,
Federal Republic of Germany

G. Alexander, G. Bella, Y. Gnat, J. Grunhaus
Tel-Aviv University²¹, Ramat Aviv, Tel-Aviv 699 78 Israel

H. Junge, K. Kraski, C. Maxeiner, H. Maxeiner,
H. Meyer, D. Schmidt

Universität-Gesamthochschule Wuppertal³, D-5600 Wuppertal,
Federal Republic of Germany

¹² Present address: Universität Karlsruhe, D-7500 Karlsruhe, FRG

¹³ Present address: CERN-EP, CH-1211 Geneva 23, Switzerland

¹⁴ Present address: University of Massachusetts, Amherst,
MA 01003, USA

¹⁵ Present address: Cosmic Ray Astrophysics Branch, Code 4154.8,
U.S. Naval Research Laboratory, Washington, DC 20375, USA

¹⁶ Present address: Texas Accelerator Center, 2319 Timberland
Place, The Woodlands, TX 77380, USA

¹⁷ Partially supported by the Department of Energy, USA

¹⁸ Present address: Instituto di Fisica, Universidad Federal do Rio
de Janeiro, Ilha do Fundao, Rio de Janeiro, RJ, Brazil

¹⁹ Present address: Universidad Autonoma de Madrid, Canto
Blanco, Madrid 34, Spain

²⁰ Present address: BESSY, D-1000 Berlin

²¹ Partially supported by the Israeli Academy of Sciences and Hu-
manities, Basic Research Foundation

Abstract. In the analysis of the reaction $e^+e^- \rightarrow e^+e^-K_S^0K_S^0$ clear evidence for exclusive $\gamma\gamma \rightarrow f_2'$ resonance production is observed. The product $\Gamma_{\gamma\gamma} \cdot B(f_2' \rightarrow K\bar{K})$ is measured to be $0.10^{+0.04+0.03}_{-0.03-0.02}$ keV independent of an *a priori* assumption on the helicity structure. Our data are consistent with a pure helicity 2 contribution and we derive an upper limit for the ratio $\Gamma_{\gamma\gamma}^{(0)}/\Gamma_{\gamma\gamma}$. The absence of events in the mass region around 1.3 GeV clearly proves destructive f_2-a_2 interference and allows to measure the relative phases between f_2 , a_2 and f_2' . Upper limits on the production of the glueball candidate states $f_2(1720)$ and $X(2230)$ as well as the $K_S^0K_S^0$ -continuum are given.

In this letter we present an analysis of the reaction $\gamma\gamma \rightarrow K_S^0K_S^0$. Special emphasis is devoted to the possible excitation of the tensor meson states $f_2(1270)$, $a_2(1320)$, $f_2'(1525)$, $f_2(1720)$ (formerly $\theta(1690)$) and $X(2230)$ (formerly $\xi(2220)$). This channel has previously been analyzed by the TASSO Collaboration [1, 2]. Preliminary results also have been reported from MARK II [3] and CELLO [4]. The f_2' radiative width has also been measured by the DELCO [5] and TPC/Two Gamma [6] Collaborations using the decay into charged kaons. Measurements of tensor meson radiative widths are important to test the validity of $SU(3)$ symmetry and are often used to determine the octet singlet mixing angle in the 2^{++} nonet. Together with measurements of the helicity structure they can test explicit production models (see e.g. [7]). A small two photon coupling of states copiously produced in radiative J/ψ decays favours their interpretation as glueballs [8].

The data were taken with the PLUTO detector at the e^+e^- -storage ring PETRA at an average beam energy of 17.43 GeV and correspond to an integrated luminosity of 45 pb^{-1} . Details of the PLUTO detector have been given elsewhere [9]. For this analysis we use track information from the central track detector and the two forward spectrometers. Electrons and photons are measured in the small angle tagger, the large angle tagger, the barrel and endcap calorimeters.

Identifying the K_S^0 by their decay into $\pi^+\pi^-$, we look for events with two positive and two negatively charged tracks to isolate the final state $K_S^0K_S^0$. Events containing photons are rejected by demanding that no isolated shower with energy larger than 100 MeV is detected. Both untagged and tagged events are accepted. At this stage the event sample is very much dominated by the reaction $\gamma\gamma \rightarrow \rho^0\rho^0$.

We now proceed with two different analyses: The

first is optimized to find K_S^0 -pairs at large production angles and is achieved by the reconstruction of the K_S^0 decay vertices in the central detector. In the second analysis K_S^0 -pairs with small production angles are selected. Here we take advantage of the PLUTO forward spectrometers and use a special procedure to avoid combinatorial background. This second path is essential for an experimental distinction between helicity 0 and 2 production mechanisms.

For the large angle K_S^0 -pair selection we search for secondary vertices using a slight modification of an algorithm previously employed in the analysis of the reaction $e^+e^- \rightarrow e^+e^-K_S^0K_S^0\pi^\pm\pi^\mp$ [10]. The algorithm searches for oppositely charged pairs of tracks in the central detector which intersect at a point with positive $r\phi$ -raw decay length. This quantity is defined as the component parallel to the track momentum sum of the distance between the track intersection point and the interaction point. The latter has been determined from Bhabha scattering for each run. All such candidates (up to 4 per event) are sorted in the order of decreasing raw decay length and fitted to the V^0 hypothesis taking into account the position of the secondary vertex and the momentum direction of the V^0 , both in the $r\phi$ and rz -projections. If a fit results in an $r\phi$ -decay length of more than 2 mm at a χ^2 of less than 12 for 3 degrees of freedom, the candidate is accepted as V^0 . Further candidates which contain one of the tracks of the accepted V^0 are rejected. The invariant mass and the momentum of the V^0 are calculated from the sum of the two track momenta evaluated at the secondary vertex assuming pion masses. The $\pi^+\pi^-$ -mass resolution obtained with this procedure is 20 MeV at the K_S^0 -mass (see [10]).

507 events are found with two accepted V^0 s, most still being background. Events containing converted photons are recognized by a (fitted) $r\phi$ -decay length consistent with the beam pipe radius or larger and an invariant e^+e^- -mass of less than 250 MeV. If all four tracks are consistent within 3 standard deviations with originating from the interaction point in $r\phi$ and a common point in z , the event is also rejected. We further demand that both decay lengths in units of their standard deviations are at least 1, and the sum of the squares of these quantities is larger than 10. Finally only V^0 s are accepted, which travelled at least 15% of the mean decay length of a K_S^0 with the measured momentum.

To select exclusive events we demand that the square of the total transverse momentum is lower than 0.08 GeV^2 . 19 events survive all these cuts, of which 10 are clearly $K_S^0K_S^0$ events, defined by a signal region of radius 50 MeV in the $\pi^+\pi^-$ -mass scatter plot of the two V^0 -candidates. From the surrounding

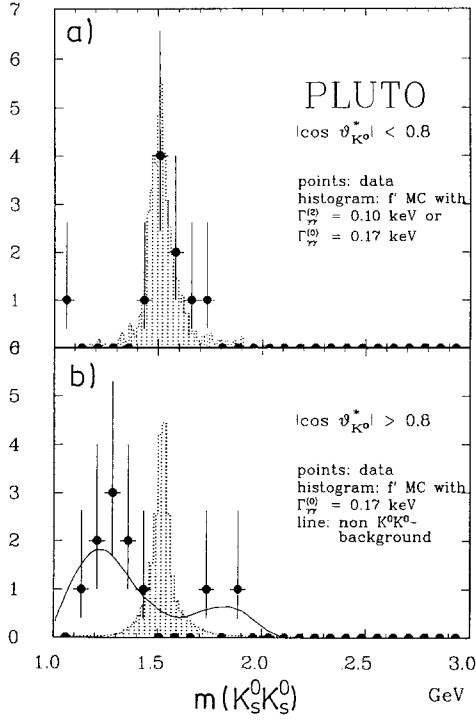


Fig. 1. **a** Invariant $K_S^0 K_S^0$ -mass spectrum for events with $|\cos\theta_K^*| < 0.8$. The shaded histogram represents the Monte Carlo expectation for exclusive f_2 production with $\Gamma_{\gamma\gamma}(f_2) \cdot B(f_2 \rightarrow K\bar{K}) = 0.10$ keV via helicity 2. The same spectrum is obtained for helicity 0 and $\Gamma_{\gamma\gamma}(f_2) \cdot B(f_2 \rightarrow K\bar{K}) = 0.17$ keV. **b** Invariant $K_S^0 K_S^0$ -mass spectrum for events with $|\cos\theta_K^*| > 0.8$. The solid line is the background estimate due to non- $K_S^0 K_S^0$ events. The shaded area denotes the expectation for f_2 resonance production, if the central detector signal is assumed to originate from helicity 0 only

region the background is calculated as 1.2 ± 0.6 events. The invariant $K_S^0 K_S^0$ mass spectrum of the 10 candidates is shown in Fig. 1a. There is one (tagged) event near the $K_S^0 K_S^0$ threshold; all other events have masses around 1.5 GeV and are taken to come from exclusive f_2 resonance production.

We now describe the second analysis path which aims at the identification of events with small f_2 decay angles. The transverse momentum of such K_S^0 being small, a secondary vertex reconstruction in the $r\phi$ -plane is not possible. Instead we select events with exactly 4 charged tracks which are compatible with originating from the interaction point. Especially important for this analysis are events with one or more tracks reconstructed in the forward spectrometers. Without secondary vertex reconstruction there are two possibilities to combine two positive and two negative tracks into two neutral pairs. In the following, however, only one combination is used, namely that which results in a smaller angle between each $\pi^+ \pi^-$ -pair momentum sum and the $\gamma\gamma$ -axis in the $\pi^+ \pi^+ \pi^- \pi^-$ -c.m.s. In untagged events the $\gamma\gamma$ -axis is approximated by the $e^+ e^-$ -axis.

Monte Carlo studies (see below) show that this algorithm is able to find the correct combination for events which really have small f_2 decay angles, producing a clear $K_S^0 K_S^0$ signal in the $\pi^+ \pi^-$ -mass scatter plot obtained with the selected paired tracks. The Monte Carlo study also proves that for these candidates the decay angle is well reconstructed with a standard deviation $\sigma(|\cos\theta_K^*|) \approx 0.01$. Again we define a signal region of radius 50 MeV and consider all events in this region and with a reconstructed $|\cos\theta_K^*| > 0.8$ as forward K_S^0 -pair candidates. The application of this procedure to the data however results in no significant signal in the $K_S^0 K_S^0$ region. Selecting exclusive events by restricting the square of the total transverse momentum to values below 0.04 GeV², we obtain 11 events in the signal region. The surrounding region gives 12.5 expected background events. The invariant $K_S^0 K_S^0$ mass spectrum of the forward K_S^0 -pairs is shown in Fig. 1b along with an estimation of the background spectrum. Observing no evidence for forward K_S^0 -pairs we use this result to derive upper limits for the production of tensor mesons via helicity 0 amplitudes.

In the following we analyse the untagged $K_S^0 K_S^0$ mass spectra obtained by the two selections in order to extract information about resonance parameters of the tensor meson states $f_2(1270)$, $a_2(1320)$, $f_2(1525)$, $f_2(1720)$ and $X(2230)$. The two photon coupling to $J^{PC} = 2^{++}$ states can be described by 5 independent form factors [11]. Adopting the form factor definition given by Poppe [7], only two of them, $F_{TT_0}(Q_1^2, Q_2^2)$ and $F_{TT_2}(Q_1^2, Q_2^2)$, describing the coupling of two transversely polarized photons to helicity 0 and 2, contribute to the radiative width^{*}:

$$\Gamma_{\gamma\gamma}(W) = \underbrace{\frac{1}{80\pi \cdot m} F_{TT_2}^2(0, 0)}_{\Gamma_{\gamma\gamma}^{(2)}} + \underbrace{\frac{1}{120\pi \cdot m} W^4 \cdot F_{TT_0}^2(0, 0)}_{\Gamma_{\gamma\gamma}^{(0)}(W)} \quad (1)$$

where m denotes the mass of the tensor meson. In the following the symbol $\Gamma_{\gamma\gamma}$ refers to the energy independent nominal radiative width of (1) evaluated at the resonance mass $W=m$. The corresponding helicity amplitudes have the form

$$M_{++} = F_{TT_0}(Q_1^2, Q_2^2) \cdot \frac{2}{\sqrt{6}} \frac{(W^2 + Q_1^2 + Q_2^2)^2 - 4Q_1^2 Q_2^2}{W^2},$$

$$M_{+-} = F_{TT_2}(Q_1^2, Q_2^2). \quad (2)$$

^{*} We treat the form factors F_{ij} as functions of Q_1^2 and Q_2^2 only (see e.g. [7, 11]). However, similarly to hadronic decay form factors, at least F_{TT_0} must exhibit some W dependence, since otherwise the elastic $\gamma\gamma$ -cross section via a tensor meson in the helicity 0 state would violate unitarity. In the absence of a “standard” prescription and because of the insensitivity of our results to the exact parametrisation we neglect this dependence

The other three helicity amplitudes involve longitudinal photons and vanish for $Q^2 \rightarrow 0$; they are neglected for the untagged events ($\langle Q^2 \rangle \approx 0.008 \text{ GeV}^2$ assuming a ρ -pole-like Q^2 dependence of the form factors). The cross section for tensor meson production and subsequent decay into $K\bar{K}$ can thus be written as

$$\sigma_{\gamma\gamma \rightarrow K\bar{K}}(W) = \frac{40\pi}{W^2} \cdot (|A_0|^2 + |A_2|^2) \quad (3)$$

with

$$A_0 = BW(W) \cdot \left(\frac{W}{m}\right)^2 \cdot (\Gamma_{\gamma\gamma}^{(0)} \cdot B(K\bar{K}))^{\frac{1}{2}}; \quad (4)$$

$$A_2 = BW(W) \cdot (\Gamma_{\gamma\gamma}^{(2)}) \cdot B(K\bar{K})^{\frac{1}{2}}$$

being the helicity 0 and 2 amplitudes respectively. $BW(W)$ denotes the relativistic Breit Wigner amplitude $BW(W) = m\sqrt{\Gamma(W)}/(W^2 - m^2 + im\Gamma(W))$ with an energy dependent width

$$\Gamma(W) = \Gamma(m) \cdot (k^*(W)/k^*(m))^5 \cdot (m/W) \cdot f^2(W)/f^2(m).$$

The energy variation of the decay form factor is assumed* to be $f^2(W) \propto (9 + 3(k^*r)^2 + (k^*r)^4)^{-1}$ [12], where k^* denotes the K_S^0 momentum in the c.m.s. of the decaying resonance and the effective interaction radius r is taken to be 1 fm. For the analysis of different resonances and interference effects Monte Carlo events have been generated with a flat K_S^0 angular distribution in the $\gamma\gamma$ c.m.s. and a fixed $\gamma\gamma$ -cross section $\sigma_{\gamma\gamma}^{MC}$ for invariant masses from $K\bar{K}$ -threshold to 3 GeV. For the photon flux we use the exact formulae given by Budnev et al. [13]. The events are passed through a detailed detector simulation program which includes a simulation of the K_S^0 decay after a finite path length in the detector and also the energy loss and multiple scattering in the detector material. Event reconstruction and selection then proceed as for real data, starting from simulated wire hits and deposited energies in the shower counters. Resonance parameters (denoted as x_i) such as radiative widths, helicity ratios and relative phases between several resonances now are determined by weighting the MC-events with a factor $\sigma_{\gamma\gamma}^{\text{Res}}(W, \cos\theta, \dots; x_i)/\sigma_{\gamma\gamma}^{MC}$ such that optimal agreement between the experimental spectra and the corresponding weighted Monte Carlo expectation is obtained.

The only visible structure in the experimental mass distribution is around 1.55 GeV and is well described by exclusive $f_2'(1525)$ -production. We take f_2' candidate events ($1.35 \text{ GeV} < m_{K\bar{K}} < 1.7 \text{ GeV}$) with

* The validity of this ansatz from nonrelativistic potential theory in this reaction is questionable. However, it describes the desired damping of the amplitude at high W . At the present level of accuracy the numerical results are insensitive to the exact form of the parametrisation

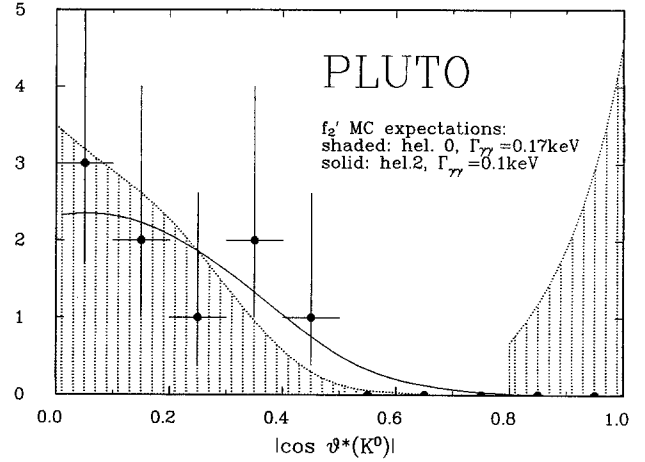


Fig. 2. f_2' decay angle distribution in the f_2' -c.m.s. The information in the region below and above $|\cos\theta_K^*| = 0.8$ is obtained by two different selections (see text). The solid curve denotes the MC expectation for helicity 2, the shaded area for helicity 0. Both expectations are normalized such that they fit the central angular region

$|\cos\theta_K^*| < 0.8$ from the central detector selection and $|\cos\theta_K^*| > 0.8$ from the forward K_S^0 pair selection to obtain the decay angular distribution shown in Fig. 2 (in fact there is one forward candidate event, where we expect a background of 2.5 events). As indicated by the curves, one respectively needs a radiative f_2' width of $0.17 \pm 0.05 \text{ keV}$ or $0.10 \pm 0.03 \text{ keV}$ to fit the central detector distribution if pure helicity 0 or pure helicity 2 production is assumed. A distinction between the two possibilities in only the central region is not possible, since both distributions differ mainly in normalisation and only little in shape. Measurements reported up to now [1, 3, 5] have needed to rely on theoretical arguments [14] and experimental results on f_2 and a_2 production, that the helicity 2 amplitude dominates at small Q^2 and neglect any helicity 0 contribution. The present forward K_S^0 -pair measurement constitutes the first *experimental* evidence for helicity 2 dominance in $\gamma\gamma \rightarrow f_2'$ production.

A fit to the angular distribution (explicitly taking into account signal and background contribution in the forward region) leads to the negative value

$$\Gamma_{\gamma\gamma}^{(0)}(f_2') \cdot B(f_2' \rightarrow K\bar{K}) = -0.03 \pm 0.03 \text{ keV}. \quad (5)$$

Restricting the result to the physical region, we obtain a Poisson upper limit for the helicity 0 radiative width:

$$\Gamma_{\gamma\gamma}^{(0)}(f_2') \cdot B(f_2' \rightarrow K\bar{K}) < 0.10 \text{ keV at 95\% c.l.} \quad (6)$$

and for the relative helicity 0 contribution:

$$\Gamma_{\gamma\gamma}^{(0)}(f_2')/\Gamma_{\gamma\gamma}(f_2') < 0.60 \text{ at 95\% c.l.} \quad (7)$$

The result for the total f_2' width is

$$\begin{aligned} & \Gamma_{\gamma\gamma}(f_2') \cdot B(f_2' \rightarrow K\bar{K}) \\ &= 0.10^{+0.04}_{-0.03}(\text{stat.})^{+0.03}_{-0.02}(\text{syst.}) \text{ keV}. \end{aligned} \quad (8)$$

This does not depend on any *a priori* assumptions on the helicity structure. The systematic error is estimated from uncertainties in luminosity measurement (3%), trigger efficiency (10%), reconstruction efficiency (e.g. hadronic interactions in the beam pipe) (10%), background subtraction (5%) as well as the effect of changing kinematic cuts (10%). Also included is a possible contribution resulting from the small helicity 0 component not excluded by our procedure described above. In what follows we show that interference with f_2 , a_2 and $f_2(1720)$ may alter $\Gamma_{\gamma\gamma}(f_2')$ considerably. The value given in Eq. 8 remains the most probable value, but the systematic error has to be increased to $^{+0.05}_{-0.04}$ keV if one allows arbitrary phases

and a non-negligible $f_2(1720)$ radiative width. The result is in good agreement with previous experiments [1, 3–6] and justifies their assumption of helicity 2 dominance.

Although the f_2' is the only structure seen in the data, we are able to make quantitative statements also about f_2 and a_2 production. Taking measured $\gamma\gamma$ partial widths and $K\bar{K}$ branching ratios from the Particle Data Group [15] we would expect to see $3.7f_2$ and $2.4a_2$ events (dashed line in Fig. 3) in the

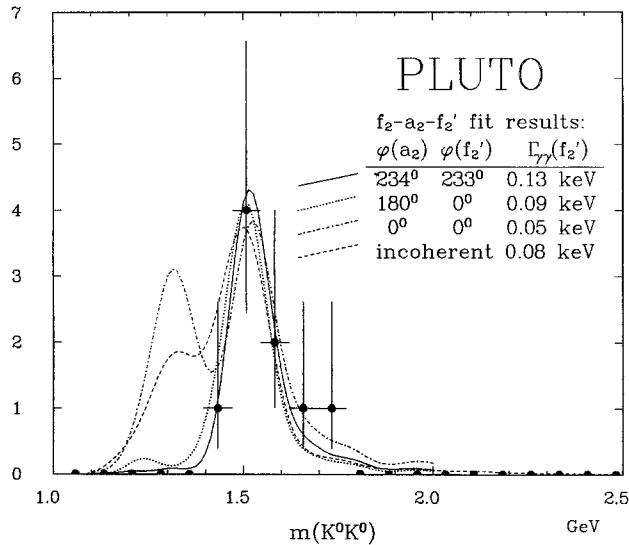


Fig. 3. Invariant $K_S^0 K_S^0$ -mass spectrum for no-tag events with $|\cos\theta_K^*| < 0.8$. The best fit to the spectrum (see text) is indicated by the solid line. The dotted line represents the expectation for destructive f_2 - a_2 and constructive f_2 - f_2' interference and also gives a good fit. Constructive interference (dash-dotted line) and incoherent addition (dashed line) describe the data much worse

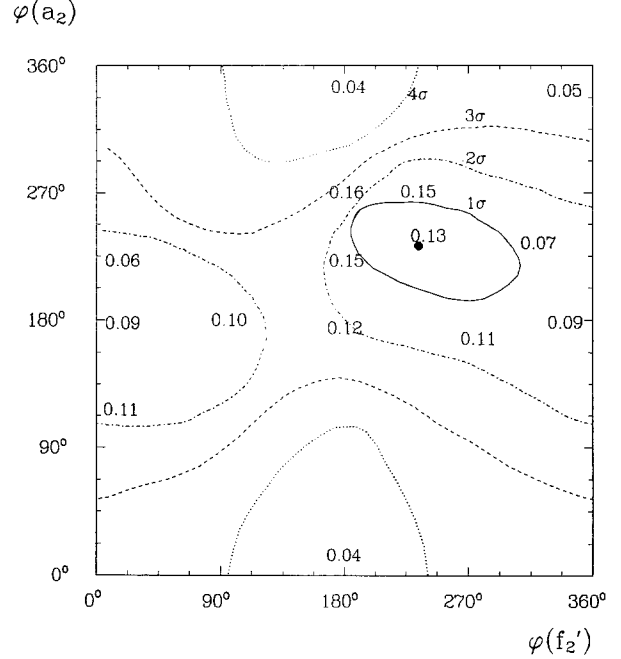


Fig. 4. Likelihood contours in the φ_{a_2} - $\varphi_{f_2'}$ plane from interference fit. Also given are best fit values for $\Gamma_{\gamma\gamma}(f_2') \cdot B(f_2' \rightarrow K\bar{K})$ [keV] at some points

case of incoherent superposition. Coherent addition of f_2 , a_2 and f_2' amplitudes with a suitable choice of phases, however, results in much better agreement with the data. Defining the amplitude as

$$A = A_f + \exp(i\varphi_{a_2}) \cdot A_{a_2} + \exp(i\varphi_{f_2'}) \cdot A_{f_2'} \quad (9)$$

we have fitted the central angular region mass spectrum between 1.1 GeV and 1.7 GeV using a maximum likelihood procedure and assuming Poisson statistics. The coupling strengths $\Gamma_{\gamma\gamma} \cdot B(K\bar{K})$ for the f_2 and a_2 are allowed to vary in the fit, contributing to the likelihood function as additional measurements with mean values and Gaussian errors taken from [15]. The radiative f_2' width is treated as a free parameter. In this fit we assume pure helicity 2 coupling for all three resonances. The best fit is obtained for:

$$\begin{aligned} \varphi_{a_2} &= \left(234^{+32}_{-36}(\text{stat.}) \pm 20(\text{syst.}) \right)^\circ \\ \varphi_{f_2'} &= \left(233^{+74}_{-50}(\text{stat.}) \pm 20(\text{syst.}) \right)^\circ. \end{aligned} \quad (10)$$

Figure 4 shows the fit probability contours in the φ_{a_2} - $\varphi_{f_2'}$ parameter space. Also given are the results for $\Gamma_{\gamma\gamma}(f_2')$ at several points, which vary considerably even in the area of good fits (0.07–0.15 keV at the 1σ contour). The systematic errors include contributions from a possible small mass calibration error not

described by the Monte Carlo simulation, a change of the total resonance widths within their experimental errors [15] and the different possible parametrisations of their energy dependence. Assuming the same phases for all $\langle 2^{++} | K\bar{K} \rangle$ couplings, Lipkin [16] has shown that in contrast to the K^+K^- final state the $a_2 \rightarrow K^0\bar{K}^0$ amplitude receives an extra minus sign from isospin. This destructive interference ($\varphi_{f'_2}=0$ ($=360^\circ$), $\varphi_{a_2}=180^\circ$) is indicated by the dotted curve in Fig. 3 and results in a reasonably good fit. Constructive interference between f_2 and a_2 (dash-dotted curve) and incoherent superposition can clearly be ruled out.

Besides the f'_2 events we observe no evidence for nonresonant $K_S^0 K_S^0$ production. From this an upper limit of the $\gamma\gamma$ cross section assuming helicity 2 dominance is derived:

$$\sigma(\gamma\gamma \rightarrow K^0\bar{K}^0) < 0.7 \text{ nb at } 95\% \text{ c.l.} \\ \text{for } 1.7 \text{ GeV} < W < 3 \text{ GeV.} \quad (11)$$

This limit still is well above the QCD prediction of Brodsky and Lepage [17].

We now derive an upper limit for the $\gamma\gamma$ coupling of the glueball candidate state $f_2(1720)$ (formerly $\theta(1690)$). As in the case of the f'_2 , previous measurements were only able to measure large angle K_S^0 -pair production. Hence the limits quoted are valid only for helicity 2 couplings and have to be multiplied by roughly a factor 2 if one also allows helicity 0 couplings [2]. The mass and width of the $f_2(1720)$ are taken from [18] to be 1.716 GeV and 0.134 GeV respectively. Combining central and forward event selection in the mass range from 1.55 to 1.9 GeV results in the relation:

$$\frac{\Gamma_{\gamma\gamma}^{(2)}(f_2(1720))}{0.07} + \frac{\Gamma_{\gamma\gamma}^{(0)}(f_2(1720))}{0.09} \\ < 1.0 \text{ keV}/B(f_2(1720) \rightarrow K\bar{K}) \text{ at } 95\% \text{ c.l.} \quad (12)$$

including 20% systematic error in the acceptance calculation. From this one gets

$$\Gamma_{\gamma\gamma}(f_2(1720)) \cdot B(f_2(1720) \rightarrow K\bar{K}) \\ < 0.07 \text{ keV at } 95\% \text{ c.l. (for helicity 2)} \quad (13)$$

or

$$\Gamma_{\gamma\gamma}(f_2(1720)) \cdot B(f_2(1720) \rightarrow K\bar{K}) \\ < 0.09 \text{ keV at } 95\% \text{ c.l. (for any helicity).} \quad (14)$$

If one allows for coherent $f'_2 - f_2(1720)$ superposition, a suitable choice of the relative phase can reduce the cross section in the $f_2(1720)$ region. A conservative estimate derived from a fit with unrestricted $\Gamma_{\gamma\gamma}(f'_2)$ and phase results in

$$\Gamma_{\gamma\gamma} \cdot B(\theta \rightarrow K\bar{K}) < 0.20 \text{ keV at } 95\% \text{ c.l.} \\ \text{(allowing } f'_2 - f_2(1720) \text{ interference).} \quad (15)$$

In contrast to the well established $f_2(1720)$ the existence of the $X(2230)$ (formerly $\xi(2220)$) is still a subject of controversial discussion [18, 19]. Nevertheless we also derive an upper limit for the coupling of this hypothetical state with $m=2.231$ GeV, $\Gamma=0.022$ GeV and $J=2$ [18] to two photons. Since the mass is well above all other $J=2$ resonances, interference effects can be neglected. From the non-observation of any candidate in neither the central nor the forward selection we calculate an upper limit of

$$\frac{\Gamma_{\gamma\gamma}^{(2)}(X(2230))}{0.06} + \frac{\Gamma_{\gamma\gamma}^{(0)}(X(2230))}{0.07} \\ < 1 \text{ keV}/B(X(2230) \rightarrow K\bar{K}) \text{ at } 95\% \text{ c.l.} \quad (16)$$

which leads to

$$\Gamma_{\gamma\gamma}(X(2230)) \cdot B(X(2230) \rightarrow K\bar{K}) \\ < 0.07 \text{ keV at } 95\% \text{ c.l. (for any helicity).} \quad (17)$$

Whether a particle state is primarily built of constituent quarks or gluons can be described by the quantity stickiness S introduced by Chanowitz [8]. This is defined as the ratio of $\Gamma(J/\psi \rightarrow \gamma X)$ to $\Gamma(\gamma\gamma \rightarrow X)$ with phase space factors removed. From our results presented above and additional numbers taken from [15] we get (with S_{f_2} normalised to 1):

$$S_{f_2} : S_{f'_2} : S_{f_2(1720)} : S_{X(2230)} \\ = 1 : 13 : > 28 (95\% \text{ c.l.}) : > 9 (95\% \text{ c.l.}) \quad (18)$$

The value for the $f_2(1720)$ has been calculated using (14). The differences between these numbers still are much smaller than the those of the pseudoscalar sector [20], where the $\eta(1440)$ (formerly $\iota(1440)$) has a stickiness more than 13 times higher than the second highest (η'). Given that the f'_2 is nearly pure $s\bar{s}$ one expects no larger stickiness for any other $q\bar{q}$ combination. However, an interpretation of the $f_2(1720)$ as radial excitation or $q\bar{q}g$ hybrid state still cannot be ruled out [21].

In summary we have analysed the reaction $\gamma\gamma \rightarrow K_S^0 K_S^0$ over the entire range of K_S^0 production angles. At large production angles we observe f'_2 production and destructive $f_2 - a_2$ interference. The product $\Gamma_{\gamma\gamma}(f'_2) \cdot B(f'_2 \rightarrow K\bar{K})$ is measured to be $0.10^{+0.04}_{-0.03}(\text{stat.})^{+0.03}_{-0.02}(\text{syst.})$ keV independent of theoretical input on the helicity structure. A fit to the angular distribution results in $\Gamma_{\gamma\gamma}^{(0)}(f'_2) = -0.03 \pm 0.03$ keV, thus confirming the dominance of the helicity 2 amplitude. The phases of the a_2 and f'_2 relative to

the f_2 are measured to be

$$\varphi_{a_2} = \left(234^{+32}_{-36} (\text{stat.}) \pm 20 (\text{syst.}) \right)^\circ$$

and

$$\varphi_{f_2} = \left(233^{+74}_{-50} (\text{stat.}) \pm 20 (\text{syst.}) \right)^\circ$$

in rough agreement with the quark model prediction of 180° and 360° respectively. We observe no evidence for the production of the glueball candidate states $f_2(1720)$ and $X(2230)$ and under reasonable assumptions obtain the upper limits $\Gamma_{\gamma\gamma}(f_2(1720)) \cdot B(f_2(1720) \rightarrow K\bar{K}) < 0.09$ keV at 95% c.l. and $\Gamma_{\gamma\gamma}(X(2230)) \cdot B(X(2230) \rightarrow K\bar{K}) < 0.07$ keV at 95% c.l., both valid for any helicity. However, if we allow arbitrary phases between all states involved, the upper limit for the $f_2(1720)$ must be increased to 0.20 keV and the systematic error on the f_2' radiative width to $^{+0.05}_{-0.04}$ keV. The absence of any events apart from the f_2' candidates leads to $\sigma(\gamma\gamma \rightarrow K^0 \bar{K}^0) < 0.7$ nb at 95% c.l. in the W -range between 1.7 and 3 GeV assuming helicity 2 dominance.

Acknowledgements. We wish to thank the members of the DESY directorate for the hospitality extended to the university groups. We are indebted to the PETRA machine group for having provided us very good beam conditions and the DESY computer center for their excellent performance. We gratefully acknowledge the efforts of all the engineers and technicians who have participated in the construction of the apparatus. Part of this work has been supported by the Bundesministerium für Forschung und Technologie, Bonn.

References

1. TASSO Collab., M. Althoff et al.: Phys. Lett. 121 B (1982) 216
2. TASSO Collab., M. Althoff et al.: Z. Phys. C29 (1985) 189
3. G. Gidal MARK II Colla.: Proc. VIIth International Workshop on Photon-Photon Collisions, p. 418. Paris 1986
4. CELLO Collab., H.J. Behrend et al.: Contributed Paper to the 1987 International Symposium on Lepton and Photon Interactions at High Energies, Hamburg, 1987
5. R.P. Johnson (DELCO Collab.): Ph.D. Thesis, SLAC-294, 1986
6. TPC/Two Gamma Collab., H. Aihara et al.: Phys. Rev. Lett. 57 (1986) 404
7. M. Poppe: Int. J. Mod. Phys. A1 (1986) 545
8. M. Chanowitz, Proc. VIth International Workshop on Photon-Photon Collisions, p. 95. Granlibakken, Lake Tahoe 1985
9. See PLUTO Collab., Internal Report DESY-PLUTO 79/01 (PRC 79/06), L. Criegee, G. Knies: Phys. Rep. 83 (1982) 153; R.G. Kellogg et al.: Internal Report DESY-PLUTO-84/04 (1984); S.L. Cartwright: Ph.D. Thesis, Internal Report DESY-PLUTO-84/01 (1984)
10. PLUTO Collab., Ch. Berger et al.: Phys. Lett. 167 B (1986) 120
11. G. Köpp, T. Walsh, P. Zerwas: Nucl. Phys. 70 B (1974) 461
12. H. Pilkuhn, in Landolt-Börnstein, New Ser. Vol. 6. Berlin, Heidelberg, New York: Springer 1972; J.M. Blatt, V. Weisskopf: Theoretical nuclear physics. New York: Wiley 1952
13. V.M. Budnev, I.F. Ginzburg, G.V. Meledin, V.G. Serbo: Phys. Rep. 15 C (1975) 181
14. P. Grassberger, P. Kögerler: Nucl. Phys. 106 B (1976) 451
15. Particle Data Group: Phys. Lett. 170 B (1986)
16. H.J. Lipkin: Nucl. Phys. 7 B (1968) 321; Procs. EPS Int. Conf. on High Energy Physics, p. 609. Palermo 1975; D. Faiman et al.: Phys. Lett. 111 B (1975) 169
17. S.J. Brodsky, G.P. Lepage: Phys. Rev. D24 (1981) 1808
18. L. Köpke (MARK III Collab.): Proc. 23rd International Conference on High Energy Physics, Berkeley 1986; University of Santa Cruz preprint SCIPP 86/74
19. A. Falvard (DM2 Collab.): Proc. VIIth International Workshop on Photon-Photon Collisions, p. 435. Paris 1986
20. B. Shen: Proc. VIIth International Workshop on Photon-Photon Collisions, p. 3. Paris 1986
21. T. Barnes: Proc. VIIth International Workshop on Photon-Photon Collisions, p. 25. Paris 1986